Synthesis of Poly(diphenylamine) Nanotubes in the Channels of MCM-41 through Self-Assembly

Kwang-Pill Lee,*,† Ali Md Showkat,† Anantha Iyengar Gopalan,†,§ Sang-Ho Kim,† and Seong-Ho Choi‡

Department of Chemistry Graduate School, Kyungpook National University, Daegu 702-701, South Korea, Department of Chemistry, Hannam University, 133-Ojung-Dong Dae duck-gu, Daejon 306-791, South Korea, and Department of Industrial Chemistry, Alagappa University, Karaikudi-630003, Tamil Nadu, India

Received June 29, 2004; Revised Manuscript Received October 4, 2004

ABSTRACT: We synthesized nanotubular poly(diphenylamine) (PDPA) by confining PDPA in the channels of MCM-41 (with a possibility of tuning the pore size). A two-stage synthesis, comprised of adsorption of diphenylamine (DPA) in the channels of MCM and subsequent oxidative polymerization to form PDPA, was employed. Adsorption of monomer was done in two different media, sulfuric acid (SA) and β-naphthalene sulfonic acid (NSA). DPA molecules form self-assembly with NSA inside the pores of MCM-41. Polymerization proceeds differently in these two selected media. NSA provides an environment for the formation nanotubular PDPA inside the pores of MCM-41. Results from nitrogen adsorption−desorption measurements, X-ray diffraction analysis, scanning electron microscopy, FTIR spectroscopy, and thermogravimetric analysis show the presence of PDPA in the channels of MCM-41. PDPA formed inside the pores of MCM-41 was also removed from the pores. Field emission transmission microscopy of PDPA extracted from the pores reveals the nanotubular morphology. FTIR spectroscopy, proton NMR spectroscopy, and conductivity measurement were used to characterize the nanotubular PDPA. The electronic state of nanotubular PDPA shows the confinement effect from MCM-41 that is different from PDPA formed by the conventional method.

Introduction

Since the discovery of mesoporous molecular sieves (MCM-41) by Kresge and Beck et al.,[1,2] this field has received much attention. The major driving forces for continuing interest on these types of materials[3−6] are the application potentialities and varieties of synthetic strategies available to prepare these types of materials. Surfactant templation has been proved to be an effective method for preparation. The procedure involves polymerization of a tetraalkoxysilane in the presence of a surfactant such as cetyltrimethylammonium bromide (CTAB). In water, the surfactant molecules can have a highly ordered structure and keep the original ordered structure even after polymer formation. Calcination or solvent washing can remove the surfactant and leave behind the silica-like polymer containing cavities or mesopores that retain the shape of the absent surfactant. Silica formed from the same starting materials (templated in the presence of a surfactant that is subsequently removed) has a periodic structure with uniform pore sizes ranging from 15 to more than 100 Å. The material termed MCM-41 possesses hexagonal symmetry in the presence or absence of surfactant.

Many different synthetic methods have been formulated and attempted for control of the size, shape, orientation, and polymorphic structure[7−9] in MCM-type materials. Various templates such as microemulsion,[10] block copolymers,[11] latex particles,[12] colloidal crystals,[13] sponge-like polymer gels,[14] and bacterial superstructures[15] have been attempted for modulating the periodicity and regularity of the porous structure in MCM-41. Also, studies have been directed to tune the pore size without affecting the structural stability of the material.[16] Use of surfactants with different hydrophobic chain lengths would induce several textural parameters for the mesoporous materials.

Inspired by the possibility of alignment of the encapsulated molecules into the host channels, different nanostructured organic−inorganic composites based on mesoporous hosts and carbon, polymer, metal, and semiconductors have been investigated.[17−24] Recently, efforts have been made on the synthesis of polyaniline (PANI), polypyrrole nanofibers, or nanotubes by chemical or electrochemical oxidative polymerization of the respective monomer. Encapsulation of nanosized conducting polymer filaments into the channels of MCM-41 hosts opened up the possibility of using mesoporous materials for making nanometer-scale electronic devices.[25−27] "Hard templates" such as aluminosilicate MCM-41[26] track-etched polymeric membranes and porous alumina and "soft templates" such as liquid crystalline phases,[28] reverse microemulsion,[29] and micelles[30,31] were used to prepare PANI, polypyrrole nanofibers, or nanotubes.

While using porous templates for making tubular or fibrous conducting polymer, each pore in the template acts as tiny reaction vessel having precise diameter and length. This type of conducting polymer nanotube/nanofiber can exhibit field emission properties for flat panel displays.[32] Recently, conducting nanotubes/fibers have been prepared by a templateless method using organic dopants.[33−36] Polymer nanotubes were formed by the in situ polymerization of self-assembly of monomer and organic dopant molecules.[33−36]

Synthesis of poly(diphenylamine), PDPA, a polymer of an N-substituted aniline derivative, received attention owing to the difference in electrochemistry, con-

* To whom correspondence should be addressed. Phone: + 82-539505901. Fax: + 82-539528104. E-mail: kplee@ knu.ac.kr.
† Kyungpook National University.
‡ Hannam University.
§ Alagappa University.

10.1021/ma048703e CCC: $30.25
Published on Web 12/30/2004

Scheme 1. Self-Assembly of Diphenylamine and β-Naphthelene Sulfonic Acid Inside the Pores of MCM-41 (A) and Nanotubular Poly(diphenylamine) Formation Inside the Pores of MCM-41 (B)

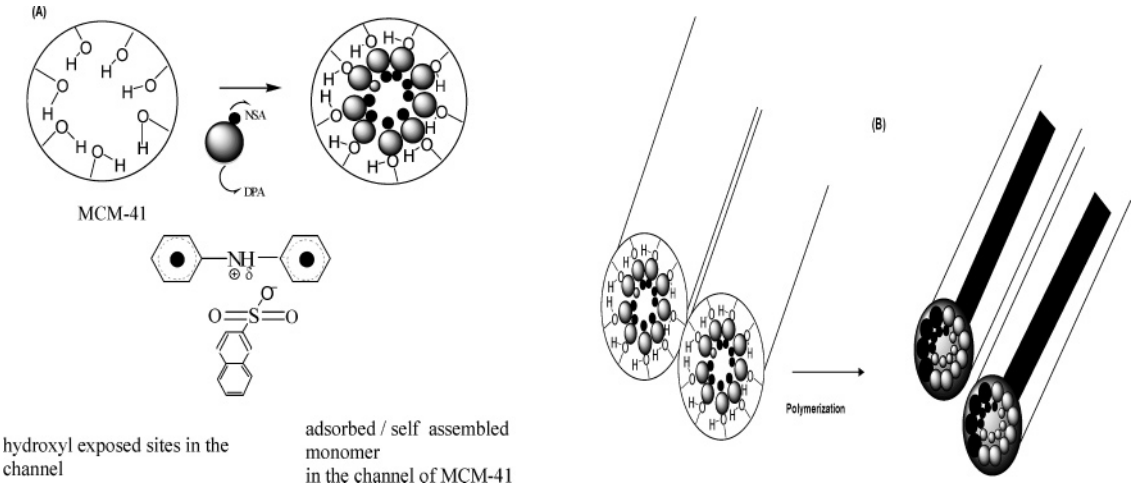

ductivity, and electrochromism[37−39] than PANI. Synthesis of PDPA in the microcavities of MCM has not been attempted so far in the presence of an organic dopant that would assist self-assembly of monomer molecules inside the cavities/pores. Such a synthesis would produce tubular conducting polymer with electronic properties that are different from the polymer prepared by the conventional method. We believe that the electronic properties of the conducting polymers can be influenced by the confinement effect induced by the inorganic host.[40,41] Hence, preparation of PDPA inside the channels of MCM-41, after self-assembly of the monomer, diphenylamine (DPA), in a dopant that can assist self-assembly in the pores, would produce PDPA with different electronic properties.

We report here the synthesis of PDPA inside the channels of MCM-41 through polymerization of the self-assembly of monomer and organic dopant in the channels. β-Naphthalene sulfonic acid (NSA), with a hydrophobic naphthalene moiety and hydrophillic sulfonate group, was used to generate self-assembly of diphenylamine (DPA) inside the pores of MCM-41. The self-assembly of DPA-NSA (Scheme 1), anchoring into the pores of MCM-41, was polymerized to produce tubular PDPA. X-ray diffraction (XRD) and N_2-adsorption measurement were used to confirm polymer formation inside the pores. FTIR spectroscopy and scanning electron microscopy (SEM) were used to characterize PDPA. Also, polymerization of DPA was performed with another dopant, sulfuric acid (SA), that cannot form self-assembly of monomer molecules in the pores. PDPA was also prepared by conventional oxidative polymerization in the absence of MCM-41. PDPA formed inside the pores of MCM-41 was extracted from the pores and characterized by proton (^{1}H) NMR spectroscopy, FTIR spectroscopy, and conductivity measurements. Field emission transmission microscopy (FETEM) was used to investigate the microstructure of the PDPA extracted from the pores of MCM-41. The properties of nanotubular PDPA formed inside the MCM-41 channel were compared with PDPA formed by the conventional method.

Experimental Section

Materials. DPA (diphenylamine), ammonium persulfate, NSA (β-naphthalene sulfonic acid), TEOS (tetraethyl orthosilicate), 1-bromoeicosane, and triethylamine were obtained from Merck and Fluka. Unless otherwise noted, all other chemicals were reagent grade and used as received.

Synthesis of MCM-41. MCM-41 was synthesized using ETAB (eicosanetrimethylammonium bromide) as surfactant by the hydrothermal procedure.[40] ETAB was prepared by the reaction of 1-bromoeicosane with triethylamine. A typical procedure for the preparation of precursor gel is outlined here. The surfactant was diluted with water and stirred for 10 min. Ammonia and ethanol were then added successively under stirring until a clear solution resulted. The surfactant solution was added dropwise to an aqueous solution of TEOS. After continuous and vigorous stirring for 210 min, a gel having the composition 0.024:0.0024:0.14:2.568:1.284 TEOS:ETAB:ammonia:water:ethanol was obtained. The gel was calcined in an oven at 550 °C. We designate the calcined materials as MCM-41. (Hexagonal packing for the MCM-41 was ascertained by X-ray diffraction analysis.[5])

Polymerization of Diphenylamine Inside the Pores of MCM-41. A 0.5 g amount of MCM-41 was dispersed in a 10 mM solution of DPA in NSA or SA, and the mixture was sonicated for 24 h with stirring. After sonication, MCM-41 was filtered, washed three times with NSA or SA, and dried to get DPA-NSA- or DPA-SA-loaded MCM-41 (designated as MCM-41(DPA-NSA) or MCM-41(DPA-SA). MCM-41(DPA-NSA) or MCM-41(DPA-SA) was placed in 20 mL of 0.5 M ammonium peroxydisulfate and stirred for 2 h at 5 °C. A dark-green-colored precipitate, NSA- or SA-doped poly(diphenylamine), PDPA-NSA or PDPA-SA loaded MCM-41 (designated as MCM-41(PDPA-NSA or MCM-41(PDPA-SA), was obtained after stirring for a few minutes. MCM-41(PDPA-NSA) or MCM-41-(PDPA-SA) was filtered, washed with distilled water, and dried at 60 °C in a vacuum oven. Separate polymerization experiments were carried out in similar conditions in NSA or SA medium without having MCM-41 in the monomer solution.

Removal of PDPA from MCM-41 Pores. MCM-41(PDPA-NSA) or MCM-41(PDPA-SA) was placed in aqueous ammonia for 24 h and stirred to dedope the PDPA-NSA. The color of the precipitate changed from green to blue during this process. The blue-colored precipitate (MCM-41 loaded with neutral PDPA) was filtered, washed with water, and dried in a vacuum oven. MCM-41 loaded with neutral PDPA was put into 20 mL of DMF and stirred for 48 h. The medium becomes blue colored, showing the removal of neutral PDPA from the pores of the MCM-41. The undissolved white mass (MCM-41) was filtered, washed with DMF, and dried in a vacuum oven. The blue-colored solution contains neutral PDPA extracted from pores of MCM-41.

Characterization. MCM-41(DPA-NSA), MCM-41(DPA-SA), MCM-41(PDPA-NSA), MCM-41(PDPA-SA), neutral PDPA extracted from MCM-41, and PDPA prepared through the conventional procedure were characterized by UV−vis spectroscopy (Shimadzu UV-2101 spectrophotometer) and FT-IR

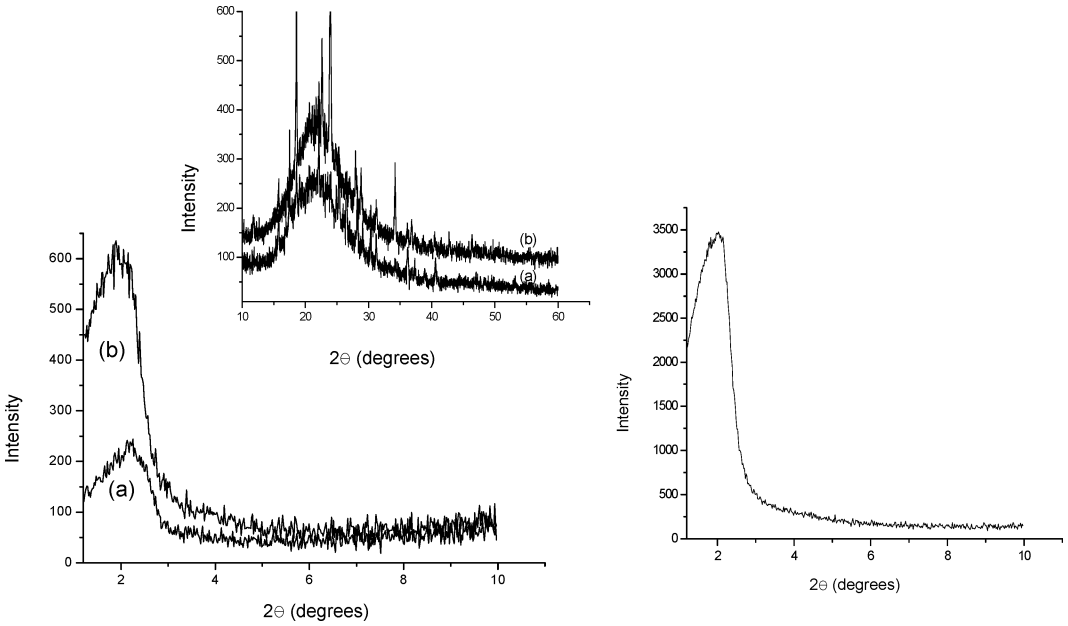

Figure 1. (A) Small-angle XRD patterns of MCM-41(PDPA-SA) (a) and MCM-41(PDPA-NSA) (b). (Inset) Wide angles. (B) Small-angle XRD pattern of pristine MCM-41.

spectroscopy (Perkin-Elmer Lamda 9N-1062 spectrometer). MCM-41(DPA-NSA), MCM-41(DPA-SA), MCM-41(PDPA-NSA), and MCM-41(PDPA-SA) were subjected to N_2 adsorption. The microstructure of PDPA extracted from MCM-41(PDPA-NSA) was investigated by means of a field emission transmission electron microscope (FETEM) (JEOL, JEM-2000EX) with a field emission electron gun operated at 200 kV. N_2 sorption (BET) measurements were carried out using a quantachrome Autosorb-1 with nitrogen as adsorbate at 77 K. The samples were degassed for 12 h at 300 °C in a vacuum before measurement. X-ray diffraction patterns were collected employing a D_8-Advanced Bruker AXS diffractometer using Cu $K\alpha_1$ radiation ($\lambda = 1.540\ 56$A°) with ($\Theta - 2\Theta$) geometry using a scintillation counter (low-angle region). The morphology of the samples was examined by scanning electron microscopy (SEM) (Hitachi, S-4200). Thermogravimetric analyses (TGA) were carried out using a TA instrument 951; ca. 0.10 mg of the sample was placed in a quartz bucket and heated at a rate of 10 °C/min in an N_2 atmosphere. Proton (^{1}H) NMR measurements were carried out on a 400 MHz Bruker, Advance Digital 400. The room-temperature conductivities of the compressed pellets of PDPA samples were determined using the conventional four-point probe method (HP 4156A Semiconductor Parameter Analyzer).

Results and Discussion

Evidence for Nanotubular PDPA Formation Inside MCM-41. PDPA was formed inside the channels of MCM-41 by performing polymerization of adsorbed monomer in two different media, NSA and SA. We could observe distinct differences in morphology, amount of polymer formed, and electronic and thermal properties, between MCM-41(PDPA-NSA) and MCM-41(PDPA-SA).

X-ray diffraction patterns of MCM-41(PDPA-NSA) and MCM-41(PDPA-SA) (Figure 1A) depict that there are distinct variations in the intensities of the peaks corresponding to the ordered structure of MCM-41 (Figure 1B) upon confining PDPA in the mesopores, and the intensity variations depend on the use of medium for the synthesis of PDPA. Besides the significant decrease in the intensity corresponding to the crystalline peak of MCM-41, an additional peak is observed for the presence of amorphous PDPA (Figure 1A, inset).

Polymerization of DPA was done by initial sorption of DPA inside the pores of MCM-41 in SA or NSA medium and subsequent chemical oxidation of the adsorbed DPA with peroxydisulfate. The physical/chemical state of DPA inside the pores in the medium of polymerization determines the morphology of PDPA.

The peak at 2.1°(2Θ), which is a signature of the highly ordered quasi-two-dimensional hexagonal lattice of MCM-41,[1,42−45] shows a significant decrease in intensity from pristine MCM-41 (Figure 1B) upon confining PDPA. The extent of decrease in peak intensity at 2.1° shows dependence on the medium of polymerization (Figure 1A) and signifies that the mechanism of PDPA formation would be different in these two media, which consequently determines the morphology of PDPA. We envisage that the self-assembly of monomer (DPA) molecules inside the pores of MCM-41 is possible and can ultimately result nanotubular PDPA. On the contrary, such a self-assembly is not possible in SA; hence, PDPA formed in SA is expected to be different. We obtained evidence for the self-assembly of DPA inside the pores of MCM-41 in NSA.

X-ray diffraction of MCM-41 adsorbed with DPA in NSA shows an additional peak at 9.99° with a concomitant decrease in the intensity of the peak corresponding to crystalline MCM-41 (Figure 2). It is presumed that the new peak corresponds to the self-assembly of DPA molecules and the probable consequent ordered structures inside the channel of MCM-41. This is an indication of short-range ordering of an anion of NSA with DPA to form self-assembly.[46] Alternatively, the new peak may be taken as an indication of the presence of an extra channel second phase. XRD measurement of MCM-41(DPA-NSA) was performed after repeated washing with water. Hence, the probability of the presence of an extra channel phase may be considered as a minimum. However, the additional peak could not be witnessed with SA. Now the reason for self-assembly of DPA with NSA in the pores of MCM-41 is explored.

The amine groups attached to the aromatic ring in DPA provide the unshared electron pair to delocalize and keep the electron as part of the aromatic ring. As a result, the aromatic units can act as a donor site for any electron-rich acceptor site. Hence, a donor−accep-

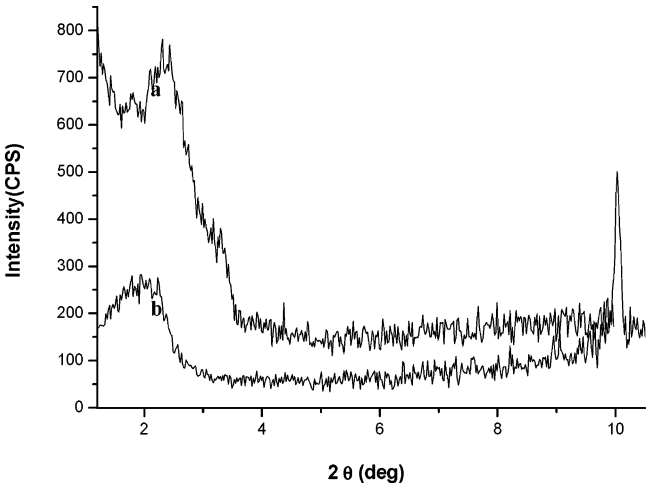

Figure 2. Small-angle XRD patterns of MCM-41(DPA-SA) (a) and MCM-41(PDPA-NSA) (b).

tor-type interaction is expected between the aromatic unit and electron-rich SiOH groups of MCM-41. During sorption of monomer, DPA is expected to be held within the framework of MCM-41 through such donor−acceptor interactions.[47] In acidic medium in the presence of NSA, protonated DPA or salt form of DPA gets attached to MCM-41 (Scheme 1) rather than the neutral DPA molecules. Additionally, the amphiphilic character of NSA due to the presence of the hydrophilic $-SO_3H$ group and lipophilic $-C_{10}H_7$ (naphthyl) groups and coexistence of NSA with its salt of DPA provide the possibility of micellar formation. With micelles consisting of NSA-DPA salt attached to MCM-41, the shell of micelles can be visualized (Scheme 1) to have a coexistence of NSA anion and diphenylamine cation in the form of electrical double layers.[48] Now the hydrophobic part of NSA can hold further layers of DPA, making a monomer-filled micellar structure attached to the pores of MCM-41. We envisage that this type of micellar structure can act like a template to form a tubular structure for PDPA. This type of micellar formation is not possible in SA, and the difference is clearly reflected on polymerization.[49−51]

There are differences in the amount of PDPA confined between MCM-41(PDPA-SA) and MCM-41(PDPA-NSA). The sorption of monomer and subsequent polymerization were carried out under similar conditions in SA and NSA. However, a weight increase of ∼16% was noticed for PDPA due to confinement in the pores of MCM-41 with NSA as the medium. In contrast, a weight increase of ∼5% was observed in the case of SA. This provides further support that during sorption monomer (DPA) molecules are held in a micellar configuration (Scheme 1) in NSA, which provides an environment able to have more monomer concentrations than in SA.

Now it is important to know whether the formed PDPA is confined in the pores or on the surface of MCM-41 sphere. To obtain this information, MCM-41(PDPA-NSA) and MCM-41(PDPA-SA) were subjected to N_2 adsorption−desorption studies. Figure 3 represents the N_2 adsorption−desorption isotherms for MCM-41(PDPA-NSA) and MCM-41(PDPA-SA). The decrease in BET surface area and pore volume (Table 1) for MCM-41-(PDPA) (for both medium) in comparison with that of pristine MCM-41 clearly shows that PDPA is predominantly present in the pores of MCM-41. MCM-41(PDPA-NSA) shows a higher decrease in surface area (99%) than MCM-41(PDPA-SA) (88%). Otherwise, only 1% pore volume of pristine MCM-41 was present after entrapment of PDPA-NSA in the pores. However, nearly 12% of the pore volume was retained in SA. These facts corroborate with the higher weight increase in NSA (∼16%) than in SA (∼5%) upon confining PDPA in the pores of MCM-41. A micellar environment with excess monomer in the matrix of MCM-41 could produce a tubular structure for PDPA in NSA and could fill the pores to a greater extent. A similar decrease in pore volume and specific surface area is observed after entrapment of polymer[26,52] or enzymes.[53]

To authenticate the tubular formation of PDPA, the polymer was extracted from MCM-41(PDPA-NSA) and the microstructure of the PDPA was examined by FETEM. Figure 4 shows a typical cross-sectional high-resolution (HR) TEM photograph of the PDPA extracted from MCM(PDPA-SA). The TEM photograph clearly provides evidence for the nanotubular morphology for PDPA (Figure 3). PDPA nanotubes with a diameter of 20−30 nm and a length of 130−180 nm could be seen (Figure 4).

On looking at the shapes of the N_2-adsorption−desorption isotherm (Figure 3) of MCM-41(PDPA-NSA) and MCM-41(PDPA-SA) it can be inferred that the pores of MCM-41 are occupied differently with PDPA-SA and PDPA-NSA. The textural difference between PDPA-SA and PDPA-NSA in the pores of MCM-41 is reflected in the adsorption hysteresis (Figure 3).

We used similar conditions to remove PDPA from the pores of MCM-41. After removal of PDPA, pore size measurements were made to obtain an idea about the regeneration of pores. While PDPA- SA could be extracted completely to regenerate the surface area as (251 m^2/g) similar to pristine MCM-41 (229 m^2/g), PDPA-NSA could not be removed fully. The MCM-41 after removal of PDPA-NSA shows 50% of the surface area as that of pristine MCM-41. The above observation also provides evidence for the tubular structure to PDPA-NSA showing difficulty for removal.

Figure 5 presents the SEM photograph of MCM-41-(PDPA-NSA) (Figure 5a) and MCM-41(PDPA-SA) (Figure 5c) and MCM-41 after removal of PDPA from the pores (Figure 5b and d). The spheres are held tightly in MCM-41(PDPA-NSA), probably by the interconnected tubular PDPA network (Figure 5a), as envisaged in Scheme 1. Otherwise, MCM spheres are threaded into tubular PDPA as noted in molecular necklace frameworks.[54] The spheres becomes less connected upon removal of PDPA from the pores.

Evidence for entrapment of PDPA inside MCM-41 pores could be obtained from comparison of the FTIR spectra of MCM-41(PDPA-NSA) (Figure 6), MCM-41-(PDPA-SA) (Figure 6), and pristine (Figure 6, inset). There are characteristic bands in the region 1300−1600 and 500−900 cm^{-1} (Figure 6) which represent the loaded PDPA in the MCM-41 pores. Typically, the band around 1400 cm^{-1} can be assigned to diphenosemiquinoaminoimine segments[37,55] in PDPA (Scheme 2), which is virtually absent in pristine MCM-41 (Figure 6, inset). Another band around 690 cm^{-1} corresponds to a C−H out-of-plane phase bending vibration of substituted benzene rings.[55] The presence of a band around 1590 cm^{-1} shows that PDPA is present in the doped form (Scheme 2). The band around 1170 cm^{-1} corresponding to a C−H bending vibration of diphenoquinone overlapping with the strong bands around 1230

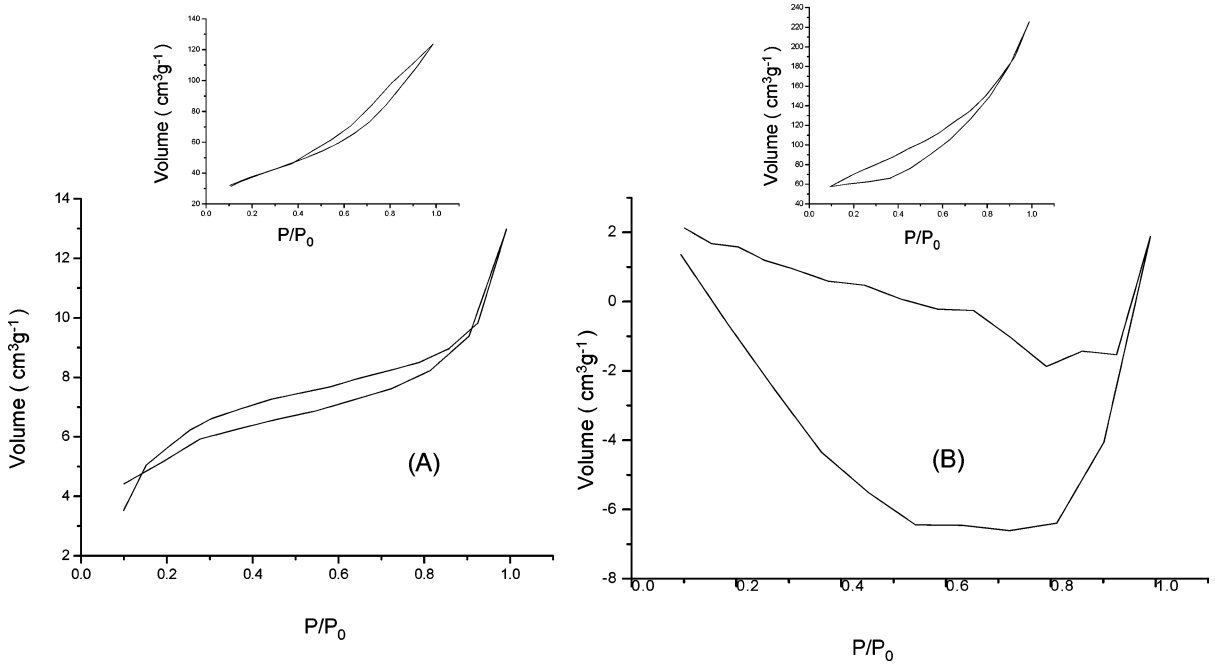

Figure 3. Nitrogen adsorption−desorption isotherms for MCM-41(PDPA −SA) (A) and MCM-41(PDPA −NSA) (B). (Inset) After removal of DPA/PDPA from the channels of MCM-41.

Table 1. BET Surface Areas, Pore Radius, Pore Volume, Cell Parameter, and Framework Thickness of Pristine MCM-41 and Confined with PDPA in the Channels

sample	specific surface area (m^2/g)	surface area (m^2)	total pore volume (m^2/g)	average pore radius (A^0)	$a_0 = 2d_{100}/\sqrt{3}(A^0)$	framework thickness (a_0-pore diameter)
pristine MCM-41	229	8.625	1. 56	12.73	49.39	23.92
MCM-41(PDPA)[a]	23.6	0.794	0.201	17.04	46.76	12.68
MCM-41(PDPA)[b]	2.48	0.054	0.003	23.38	50.77	4.019
MCM-41(PDPA)[c]	130	3.124	0.191	28.67	43.10	
MCM-41(PDPA)[d]	251	1.156	0.348	27.72	49.16	

[a] MCM-41(PDPA-SA). [b] MCM-41(PDPA- NSA). [c] MCM-41 after removal of PDPA-SA. [d] MCM-41 after removal of PDPA −NSA.

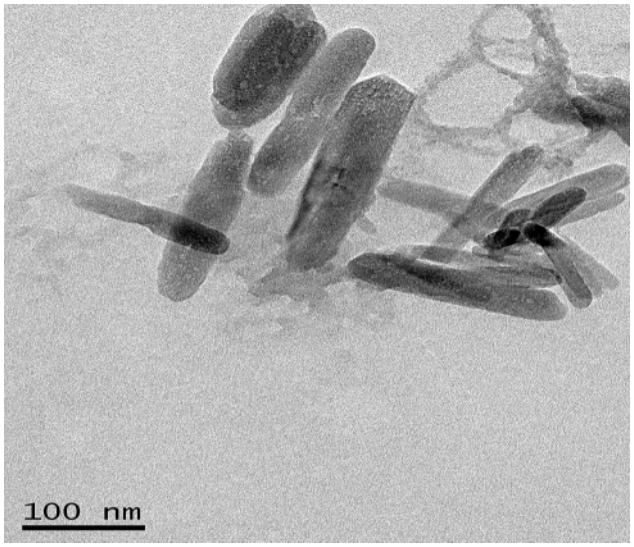

Figure 4. FETEM photograph of PDPA extracted from the pores of MCM-41.

and 1000 cm^{-1} for Si−O−Si stretching.[56,57] Similarly, the band that is predominantly observed around 3390 cm^{-1} for PDPA-confined MCM-41, corresponding to H-bonded NH stretching vibrations (Figure 6), suppresses the band around 3520 cm^{-1} for the hydroxyl group of silanol units.[56,57,47] The N−H bending vibrations in PDPA overlaps with the Si−O stretching overtone of MCM-41. The characteristic bands of PDPA showed a decreased intensity on removing PDPA from MCM-41 pores (Figure 6).

Thermograms of MCM-41(PDPA- NSA) and MCM-41(PDPA-SA) (Figure 7) clearly show the presence of PDPA. While MCM-41 exhibits thermal stability beyond 250 °C, the thermograms of MCM-41(PDPA- NSA) and MCM-41(PDPA-SA) show thermal transitions associated with PDPA.[58]

Characterization of Nanotubular PDPA. The nanotubular PDPA extracted from MCM-41(PDPA-NSA) was further characterized for structure and properties. It is important to note that extraction of nanotubular PDPA from MCM-41(PDPA-NSA) involves neutralization with aqueous ammonia. Hence, the nanotubular PDPA exists in neutral form.

FTIR spectra of nanotubular PDPA and neutralized PDPA prepared through conventional polymerization are presented (Figure 8). The nanotubular PDPA show variations in the band position and pattern corresponding to a C−H bending vibration of diphenoquinone units (~1170 cm^{-1}), a stretching vibration of diphenosemiquinoaminoimine segments (~1400 cm^{-1}), C=C stretching of benzenoid rings (~1500 cm^{-1}), and N−H stretching vibrations (~3400 cm^{-1}), in contrast to neutral PDPA prepared by the conventional method. Typically, the peaks around 1170, 1400, 1500, and 3400 cm^{-1} show splitting with the appearance of a shoulder close to the main peaks. We envisage that in the nanotubelar PDPA

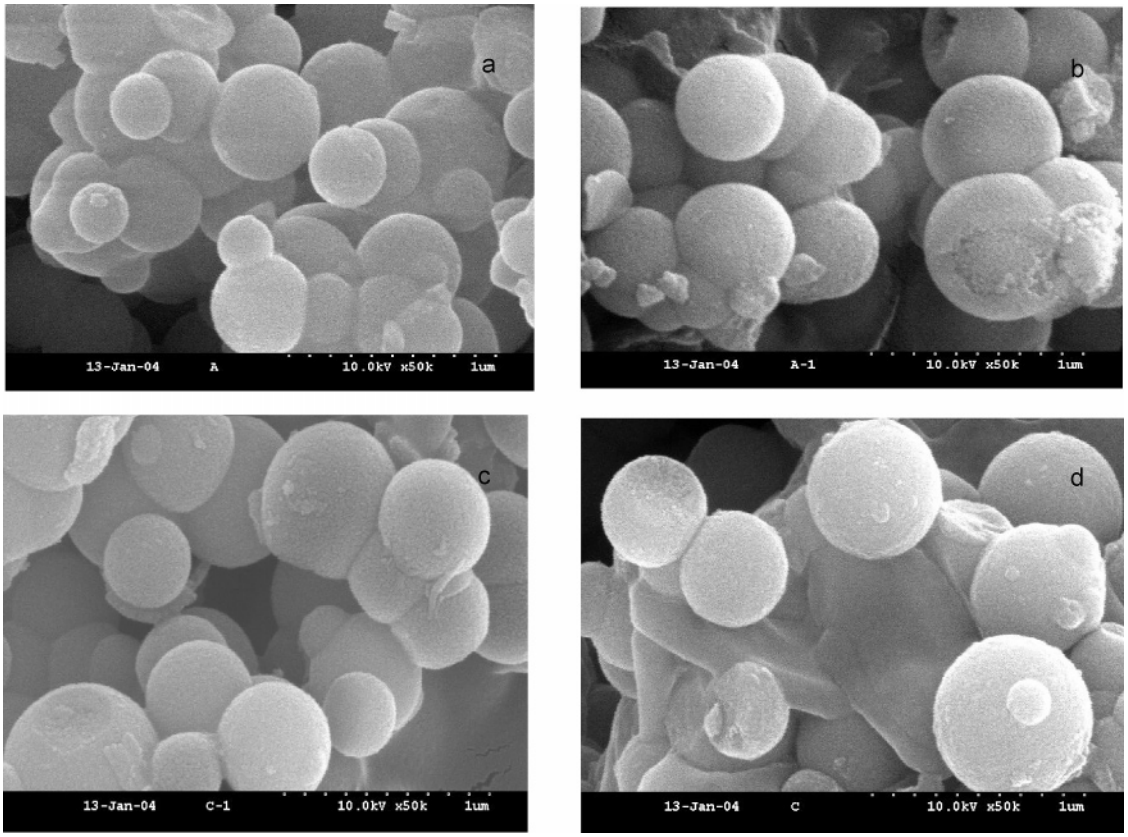

Figure 5. SEM photographs of MCM-41(PDPA-NSA) (a) and MCM-41(PDPA-SA) (c), after removal of PDPA-NSA from the pores of MCM-41 (b), and after removal of PDPA-SA from the pores of MCM-41 (d).

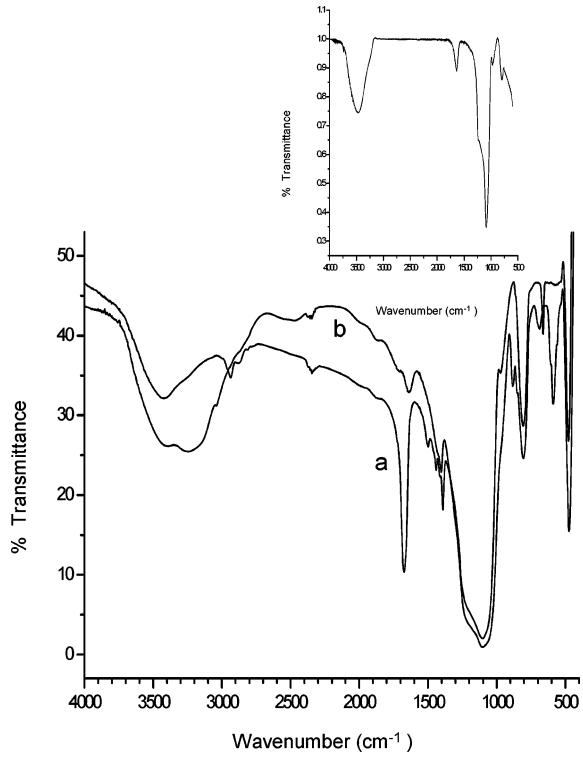

Figure 6. FTIR spectra of MCM-41(PDPA-SA) (a) and MCM-41(PDPA-NSA) (b). (Inset) MCM-41 after the removal of PDPA-SA from the pores.

Scheme 2. Redox States of PDPA

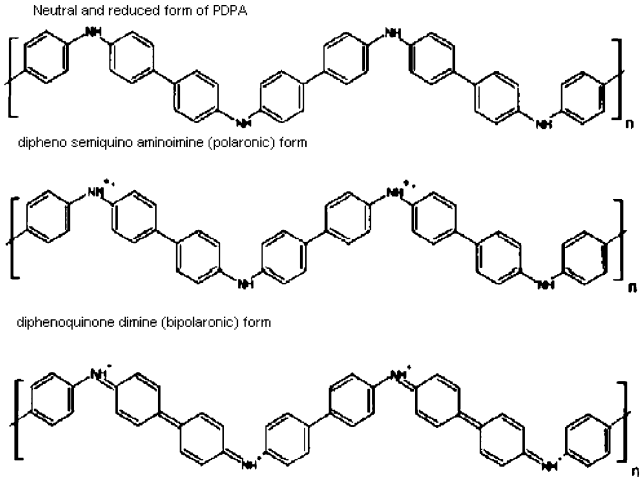

there can be intermolecular interactions between polaronic (diphenosemiquinoaminoimine), (Scheme 2) and bipolaronic (diphenoquinoneimine) (Scheme 2) forms. This would cause the splitting of the respective peaks.

The proton NMR spectrum of nanotubular PDPA, neutral PDPA prepared by the conventional method, and the monomer (DPA) are presented (Figure 9). Clearly there is a difference in the splitting pattern of the signal in the range 6.8−7.8 ppm that corresponds to the double-substituted phenyl rings of PDPA between nanotubular PDPA and conventional PDPA. Besides, the signal corresponding to the amino proton in the range 5.2−6.1 ppm, differences between nanotubular PDPA and conventional PDPA also appear. These two observations are consistent with the splitting pattern of the bands that represent the C−H bending vibration of diphenoquinoneimine (~1170 cm^{-1}), semiquinoaminoimine (~1400 cm^{-1}), and N−H stretching vibrations (~3400 cm^{-1}). These observations indicate that there can be intermolecular interactions between bipolaronic

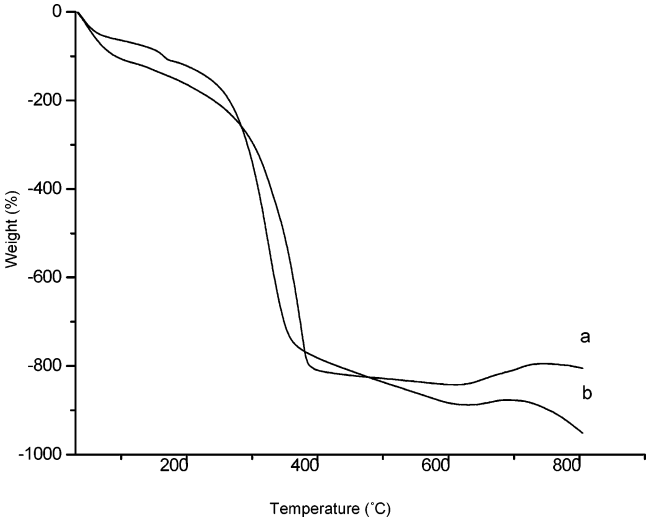

Figure 7. Thermograms of MCM-41(PDPA-SA) (a) and MCM-41(PDPA-NSA) (b).

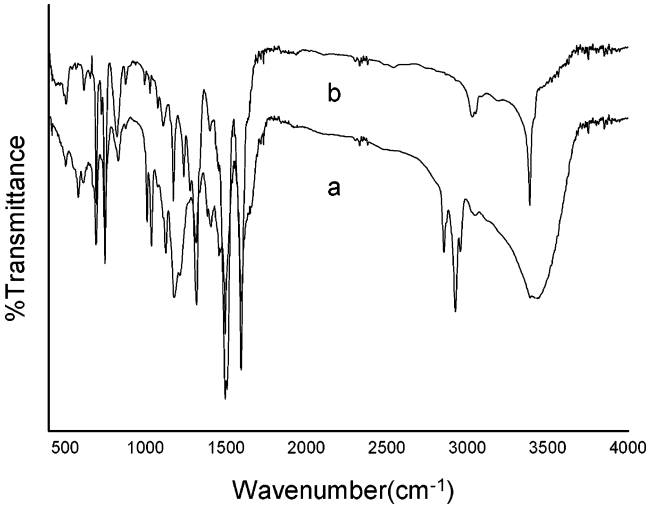

Figure 8. FTIR spectra of PDPA extracted from the pores of MCM-41 (a) and PDPA prepared by conventional polymerization (b).

and polaronic states of PDPA involving the amine and imine units of PDPA.

The room-temperature conductivity of nanotubular PDPA was found to be 8.9×10^{-4} S/cm. The conductivity of neutral PDPA prepared by oxidative polymerization was 2.23×10^{-2} S/cm. The lower conductivity for nanotubular PDPA may be ascribed to the decreased possibility of doping the PDPA chains by NSA ions. A decreased proportion of NSA to DPA molecules may be expected to be present in the self-assembly of DPA inside the MCM-41. This could ultimately restrict the extent of doping and resulting lower conductivity.

UV−vis spectroscopy was used to determine the electronic state of PDPA-SA and PDPA-NSA confined in MCM-41. Interestingly, the electronic states of PDPA-SA and PDPA-NSA are different and correlate with the textural variations between them. Figure 10 gives the UV−vis spectra of PDPA after removal from MCM-41 pores. PDPA-SA neutralized with aqueous ammonia showed a shoulder around 320 and 470 nm for the polaronic form of PDPA (Scheme 2). On the contrary, the UV−vis spectrum of the neutralized form of PDPA-NSA has a band around 570 nm which is characteristic of the diphenoquininedimine form of PDPA or bipolaronic state of PDPA.[39,55] Otherwise, PDPA-NSA formed

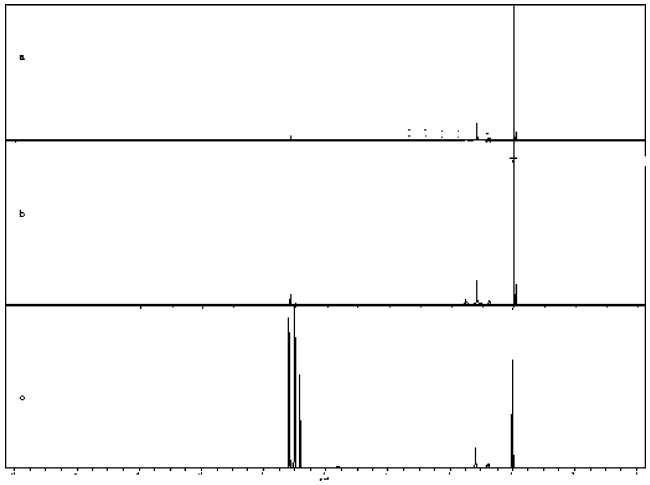

Figure 9. ^{1}H NMR spectra of PDPA extracted from the pores of MCM-41 (a), PDPA prepared by conventional polymerization (b), and diphenylamine(monomer) (c).

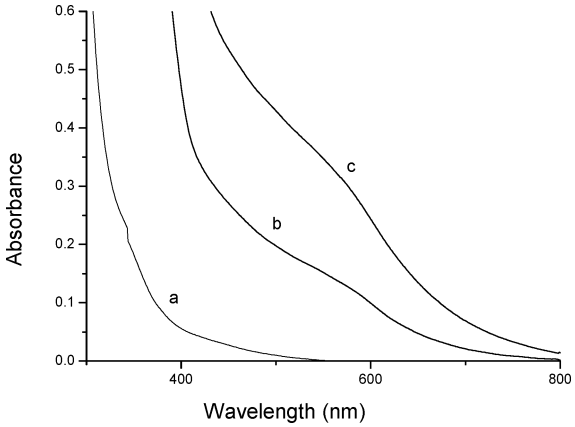

Figure 10. UV−vis spectra of neutral PDPA after removal from MCM-41(PDPA-SA) (a) and MCM-41(PDPA-NSA) formed with different monomer concentrations (b, c).

by the self -assembly of monomeric units exists in the bipolaronic state through the interband transition, even after neutralization. The existence of such interband transitions (between polaronon and bipolaron states) is in accordance with the splitting of the bands corresponding to diphenoquinonediimine and semiquinoaminoimine as inferred from FTIR spectra of nanotubular PDPA (Figure 8).

The presence of such a different electronic state for PDPA-NSA formed inside pores of MCM-41 was further verified. Toward this purpose, PDPA-NSA was prepared through normal oxidative polymerization under conditions similar to the those used for preparing PDPA inside MCM-41 pores. Figure 11 presents the UV−vis spectra of PDPA-NSA and neutralized PDPA prepared through the conventional method. The neutralized PDPA-NSA has a peak around 630 nm characteristic of the polaronic form of PDPA. However, nanotubular PDPA-NSA formed inside MCM-41 pores retains the bipolaronic state even after neutralization with a band around 570 nm. This shows that the electronic state of nanotubular PDPA formed inside the pores of MCM-41 is retained even after removal from MCM-41. Such a confinement effect induced from MCM-41 was not found for PDPA-NSA formed outside the pores. Otherwise, the electronic state of nanotubular PDPA formed inside the pores of MCM-41 is different from that of PDPA formed by conventional methods.[40,41]

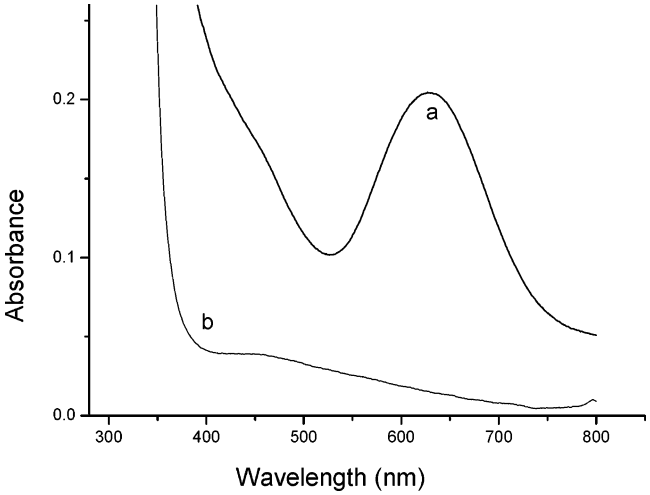

Figure 11. UV−vis spectra of PDPA prepared by conventional polymerization: (a) after neutralization with ammonia and (b) doped with NSA.

Conclusions

Nanotubular poly(diphenylamine) was formed inside the channels of MCM-41 by self-assembly of monomer molecules in the pores prior to polymerization. This approach can be successfully extended for the preparation of nanotubular polymers with other types of monomers. The observed different electronic property for nanotubular PDPA is the consequence of a confinement effect induced by mesoporous host and adds interest to take up further studies. The confinement effect can originate from weak intermolecular interactions, electron interactions, or coordination effects that could cause 'docking' of molecular units into the cavities of molecular sieves. The surface curvature of pore walls can also influence the confinement effect. Research activities are underway to investigate the confinement effect on the electronic state of the conducting polymer formed inside the pores.

Acknowledgment. This work was supported by the Korean Research Foundation Grant (KRF-2004-005-00009) and the MOST (Ministry of Science & Technology) through the CAPT (Center for Automotive Parts Technology) at Keimyung University. The authors acknowledge the assistance of the center for high volt transmission microscope, Korea Basic Science Institute, Daejon, Korea, for recording the FETEM photographs.

References and Notes

(1) Kresge, C. T.; Leonowicz, M. E.; Roth, W. J.; Vartuli, J. C.; Beck, J. C. *Nature* **1992**, *359*, 710.
(2) Sayari, A. *Stud. Surf. Sci. Catal*. **1996**, *102*, 1.
(3) Moller, K.; Bein, T. *Chem. Mater*. **1998**, *10*, 2950.
(4) Stein, A.; Melde, B. J.; Schroden, R. C. *Adv. Mater*. **2000**, *12*, 1403.
(5) Corma, A. *Chem. Rev*. **1997**, *97*, 2373.
(6) Sayari, A. *Chem. Mater*. **1996**, *8*, 1840.
(7) Heuer, A. H.; Fink, D. J.; Laraia, V. J.; Arias, J. L.; Calvert, P. D.; Kendall, K.; Messing, G. L.; Blackwell, J.; Rieke, P. C.; Thompson, D. H.; Wheeler, A. P.; Veis, A.; Caplan, A. I. *Science* **1992**, *255*, 1098.
(8) Mann, S.; Ozin, G. A. *Nature* **1996**, *382*, 313.
(9) Walsh, D.; Mann, S. *Nature* **1995**, *377*, 320.
(10) Zhao, D.; Feng, J.; Huo, Q. S.; Melosh, N.; Fedrickson, G. H.; Chemelka, B. F.; Stucky, G. D. *Science* **1998**, *279*, 548.
(11) Ono, Y.; Nakashima, K.; Sano, M.; Kanekiyo, Y.; Inoue, K.; Hojo, J.; Shinkai, S. *Chem. Commun.* **1998**, 1477.
(12) Velev, O. D.; Jede, T. A.; Lobo, R. F.; Lehnoff, A. M. *Chem. Mater*. **1998**, *10*, 3597.
(13) Breulmann, M.; Colfen, H.; Hentze, H. P.; Antonietti, M.; Walsh, D.; Mann, S. *Adv. Mater*. **1998**, *10*, 237.
(14) Archibald, D. D.; Mann, S. *Nature* **1993**, *364*, 430.
(15) Lindlar, B.; Luchinger, M.; Rothlisberger, A.; Haouas, M.; Pirngruber, G.; Kogelbauer, A.; Prins, R. *J. Mater. Chem*. **2002**, *12*, 528.
(16) Martin, T.; Galarneau, A.; Brunel, D.; Izard, V.; Hulea, V.; Blanc, A. C.; Abramson, S.; Di Renz, F.; Fajula, F. *Stud. Surf. Sci. Catal.* **2001**, *135*, 178.
(17) Kim, T. H.; Jang, L. W.; Lee, D. C.; Choi, H. J.; Jhon, M. S. *Macromol. Rapid Commun.* **2002**, *23*, 191.
(18) Bein, T.; Wu, C. G. *Chem. Mater.* **1994**, *6*, 1109.
(19) Cui, J.; Yue, Y. H.; Dong, W. Y.; Gao, Z. *Stud. Surf. Sci. Catal.* **1997**, *105A*, 687.
(20) Hartmann, M.; Poppl, A.; Kevan, L. *J. Phys. Chem.* **1995**, *99*, 17494.
(21) Hartmann, M.; Poppl, A.; Kevan, L. *J. Phys. Chem.* **1996**, *100*, 9906.
(22) Leon, R.; Margolese, D.; Stucky, G.; Petroff, P. M. *Phys. Rev.* **1995**, *B 52*, R2285.
(23) Srdanov, V. I.; Alxneit, I.; Stucky, G. D.; Reaves, C. M.; DenBaars, S. P. *Phys. Chem.* **1998**, *B102*, 3341.
(24) Agger, J. R.; Anderson, M. W.; Pemble, M. E.; Terasaki, O.; Nozue, Y. *J. Phys. Chem.* **1998**, *B 102*, 3345.
(25) Han, Y. J.; Kim, J. M.; Stucky, G. D. *Chem. Mater.* **2000**, *12*, 2068.
(26) Moller, K.; Bein, T. *Chem. Mater*. **1998**, *10*, 2950.
(27) Wu, C.; Bein, T. *Science* **1994**, *264*, 1756.
(28) Wu, C.; Bein, T. *Science* **1994**, *266*, 1013.
(29) Huang, L.; Wang, Z.; Wang, H.; Cheng, X.; Mitra, A.; Yan, Y. *J. Mater. Chem.* **2002**, *12*, 388.
(30) Jiang, J.; Yoon, H. *Chem. Commun.* **2003**, 720.
(31) Qiu, H.; Wan, M.; Matthews, B.; Dai, L. *Macromolecules* **2001**, *34*, 675.
(32) Yang, J.; Wan, M. *J. Mater. Chem.* **2002**, *12*, 897.
(33) Yang, Y.; Liu, J.; Wan, M. *Nanotechnology* **2002**, *13*, 771.
(34) Wang, C.; Wang, Z.; Li, M.; Chen, H. Li. *Phys. Lett.* **2001**, *341*, 431.
(35) Wei, Z.; Wan, M.; Li, T.; Dai, M. *Adv. Mater.* **2003**, *15*, 136.
(36) Wei, Z.; Zhang, Z.; Wan, M. *Langmuir.* **2002**, *18*, 917.
(37) Dao, L. H.; Guay, J.; Leclerc, M. *Synth. Met.* **1989**, *29*, E383.
(38) Guay, J.; Paynter, R.; Dao, L. H. *Macromolecules* **1990**, *23*, 3598.
(39) Chung, C. Y.; Wen, T. C.; Gopalan, A. *Electrochim. Acta* **2001**, *47*, 423.
(40) Zhang, L. Z.; Cheng, P.; Liao, D.-Z. *J. Chem. Phys*. **2002**, *117*, 5959.
(41) Zhang, L. Z.; Cheng, P.; Tang, G.-T.; Liao, D.-Z. *J. Luminescence* **2003**, *104*, 123.
(42) Lin, H. P.; Cheng, S.; Mou, C. Y. *Microporous Mater.* **1997**, *10*, 111.
(43) Beck, C.; Vartuli, J. C.; Roth, W. J.; Leonwicz, M. E.; Schonidit, K. D.; Chu, C. T. W.; Olson, D. H.; Sheppard, E. W.; Cullin, S. B. M.; Higgins, J. B.; Schlenteer, J. L. *J. Am. Chem. Soc.* **1992**, *114*, 10834.
(44) Selvarss, P.; Bhatie, S. K.; Sonware, C. *Ind. Chem. Eng. Res*. **2001**, *40*, 3237.
(45) Dapurkar, S. E.; Badamali, S. K. *Catal. Today* **2001**, *68*, 63.
(46) Yan, Y.; Wan, M. *J. Mater. Chem.* **2002**, *12*, 897.
(47) Eimer, G. A.; Gómez, C. M. B.; Pierella, L. B.; Anunziata, O. A. *J. Colloid Interface Sci.* **2003**, *263*, 400.
(48) Kumarato, N.; Genies, E. M. *Synth. Mater.* **1995**, *68*, 191.
(49) Hirose, G.; Sepulveda, L. *J. Phys. Chem.* **1981**, *85*, 3689.
(50) Hirous, G.; Stache, H.; Ed, W. *Anionic surfactant organic chemistry*; Marcel Dekker: New York, 1995; Vol. 56, p 82.
(51) Bockstaller, M.; Kohler, W.; Wegner, G.; Vlassopoulos, D.; Fytas, G. *Macromolecules* **2000**, *33*, 3951.
(52) Cho, M. S.; Choi, H. J.; Kim, K. K.; Ahn, W. S. *Macromol. Chem. Rapid Commum*. **2002**, *23*, 713.
(53) Takahashi, H.; Sasaki, B.; Li, T.; Miyazaki, C.; Kayns, T.; Inayaki, S. *Chem. Mater.* **2000**, *12*, 3301.
(54) Harada, A.; Li, J.; Kamachi, M. *Nature* **1992**, *356*, 325.
(55) Rajendran, V.; Gopalan, A.; Vasudevan, T.; Wen, T.-C. *J. Electrochem. Soc.* **2000**, *147* (8), 3014.
(56) Eimer, G. A.; Pierella, L. B.; Monti, G. A.; Anunziata, O. A. *Catal. Lett.* **2000**, *78*, 65.
(57) Eimer, G. A.; Pierella, L.; Annunziata, O. *Stud. Surf. Sci. Catal*. **2001**, *135*, 970.
(58) Wu, M. S.; Wen, T. C.; Gopalan, A. *Mater. Chem. Phys.* **2002**, *74*, 58.

MA048703E